Research Article

Predicting the Onset of Cavitation in Automotive Torque Converters—Part II: A Generalized Model

D. L. Robinette,[1] J. M. Schweitzer,[1] D. G. Maddock,[1] C. L. Anderson,[2] J. R. Blough,[2] and M. A. Johnson[2]

[1] *General Motors Powertrain Group, General Motors Corporation, Pontiac, MI 48340, USA*
[2] *Department of Mechanical Engineering—Engineering Mechanics, Michigan Technological University, Houghton, MI 49931, USA*

Correspondence should be addressed to D. L. Robinette, darrell.robinette@gm.com

The objective of this investigation was to develop a dimensionless model for predicting the onset of cavitation in torque converters applicable to general converter designs. Dimensional analysis was applied to test results from a matrix of torque converters that ranged from populations comprised of strict geometric similitude to those with more relaxed similarities onto inclusion of all the torque converters tested. Stator torque thresholds at the onset of cavitation for the stall operating condition were experimentally determined with a dynamometer test cell using nearfield acoustical measurements. Cavitation torques, design parameters, and operating conditions were resolved into a set of dimensionless quantities for use in the development of dimensionless empirical models. A systematic relaxation of the fundamental principle of dimensional analysis, geometric similitude, was undertaken to present empirical models applicable to torque converter designs of increasingly diverse design parameters. A stepwise linear regression technique coupled with response surface methodology was utilized to produce an empirical model capable of predicting stator torque at the onset of cavitation with less than 7% error for general automotive torque converter designs.

1. INTRODUCTION

Part I of this two-part paper discussed the principles of cavitation inception in the torque converter at stall, acoustical detection with a dynamometer test cell, and dimensional analysis for the strict case of exact geometric scaling. The focus of Part II is on the application of dimensional analysis for development of empirical models capable of predicting stator torque cavitation thresholds at stall for a wide range of torque converter designs.

The potential for cavitation exists during stall operation (converter output speed held at zero) for any torque converter above some critical torque and charge pressure. A cavitation model could be used to optimize converter designs to achieve higher cavitation torque thresholds at stall and minimize cavitation under normal driving conditions. The objective then is to increase stator torque at cavitation as a function of design parameters and flow properties, for example, pressures and cooling flow temperature, for any general automotive torque converter design.

Although the results of Part I are fundamental to the principles of dimensional analysis, they provide little practical use in predicting cavitation thresholds for a diverse population of torque converters needed to meet performance requirements in a wide range of powertrain applications. To date, a comprehensive empirical model, spanning the design space of torque converters or other turbomachines, for predicting cavitation thresholds has not been developed. Dimensional analysis using a power product model and using response surface methodology (RSM) was applied to the torque converter data to develop models for cavitation. However, it was found that the power product model did not adequately satisfy the assumption of linear regression analysis, namely, normality and constancy of error variance for model residuals. Instead, RSM was used to statistically determine the functional form of the model (dimensionless regressors) resulting in a model with better normality and constancy of error variance as well as increased prediction accuracy. RSM is a technique that is particularly well suited for the development of empirical models in which an optimal solution is sought. By definition, RSM is a mathematical and statistical approach to modeling and analysis of data to which the response of interest is influenced by several variables and the objective is to optimize the response

[1]. Application of RSM and regression techniques has previously been implemented in the design optimization of a compressor impeller [2] and turbine blades [3–5], diffusers [1], scroll fans [6], and torpedoes [7] for maximum component performance.

The formulation of a generalized torque converter cavitation prediction model requires knowledge of operating thresholds at cavitation. For this investigation, these were obtained by relaxing geometric similitude and testing a matrix of converters designs on a dynamometer setup for determination of $T_{s,i}$, stator torque at the onset of cavitation. Even with geometric similitude relaxed, similarity was preserved by maintaining consistent design philosophies for each element (i.e., pump, stator, or turbine) regardless of torus geometry. Blades for turbines and pumps are constant thickness sheet metal designs defined by inlet and outlet angles and with a ruled surface from hub to shroud. Stator blades are defined by inlet and outlet angles, and also by airfoil shapes that are similar between different angle designs. The stall hydrodynamic behavior of any one design tested is also a source of similarity. Like all turbomachines, changes to the geometry of the torque converter only modify its unique performance metrics, and not its overall function. Every converter tested exhibits a characteristic K-factor (see Part I) and stall torque ratio, the ratio of turbine to pump torque, as a function of geometry changes to one or multiple elements. Previous experimental work by [8] found that the onset of cavitation consistently correlated with the torus and element geometries of the torque converter. Given these similarities, it is expected that the use of dimensional analysis will not be hindered due to relaxed geometric similitude among the tested parts.

Nondimensional terms were determined from the important variables that describe cavitation within a torque converter at stall and were used as inputs into a RSM to form a generalized model. The resulting model is dimensionally homogenous and contains dimensionless quantities that represent meaningful relationships among the initial list of fundamental variables. A similar approach of combining RSM and dimensional analysis was demonstrated by [9] for the optimization of stresses and buckling loads of an isotropic plate with an abrupt change in thickness.

2. GENERAL CONSIDERATIONS

2.1. Element design modifications and cavitation

For any combination of internal combustion engine and automatic transmission, the performance of the torque converter must be optimized over all possible speed ratios for efficiency, torque ratio, tractive effort, vehicle acceleration, and fuel consumption. Torus dimensions and shape are usually determined first by powertrain packaging constraints, K-factor performance targets, and consideration for rotating inertia. Once the dimensions of the torus are selected, element designs are explored to refine performance over all possible speed ratios. For a given set of torus dimensions, a single turbine design is developed for use with any combination of pumps or stators to be developed. The

stamped sheet metal blades of the pump lend themselves to adjustments in inlet and outlet angles, with blade count fixed for a given diameter. The stator can be modified by changing blade angles, both inlet and outlet simultaneous, and the airfoil shape of the blade. Any change in converter diameter will scale K-factor by the ratio of the diameters to the 2.5 power, while axial length has a marginal effect. Increasing pump outlet angle will lower K-factor and torque ratio at stall, while improving efficiency at high speed ratio. Stator outlet angles of increased magnitude produce higher K-factors and lower torque ratios at stall but improve peak efficiency at high speed ratio. The airfoil shape of the stator blade influences stall torque ratio and K-factor at high-speed ratio. These design parameters that are crucial to tuning torque converter performance are also influential to cavitation characteristics and were evaluated in the dimensional analysis. Torque converter designs, with increased diameter and axial length that contain pumps and stators of low magnitude blade angles, will result in increased cavitation thresholds as described in [8]. The reader is referred to [8] for a more thorough discussion on the influence of design parameters on performance and cavitation.

2.2. Parameters for dimensional analysis

Stator torque at the onset of cavitation for any torque converter design is a function of the specific design and operating point parameters that determine the boundary value problem of the toroidal flow. The stator torque cavitation threshold, $T_{s,i}$, for any torque converter design is primarily a function of torus dimensions D and L_t, and element blade designs comprising of blade angles for pump, turbine, and stator, and blade airfoil shape for the stator. Element design parameters manifest themselves as the integrated quantities of K-factor (see Part I), K, and the ratio of turbine to pump torque, known as torque ratio, TR. Both quantities at stall correlate to cavitation behavior in the converter, see [8], and their simplicity is preferred over a lengthy and detailed list of individual blade design parameters for each element. However, the number of blades and airfoil shape of the stator can strongly influence performance and cavitation behavior and was also included. Airfoil shape is specified by the maximum blade thickness, t_{max}, and chord length, l_c. Stator blade count and shape have been shown to affect $T_{s,i}$ as described by [8]. Pressures superimposed upon the torque converter can alter $T_{s,i}$ by as much as 150 Nm as determined by [8] and are considered primary variables. As in Part I, average pressure, p_{ave}, and pressure drop, Δp, are more suitable to the dimensional analysis than charge and back pressures.

Secondary variables that influence $T_{s,i}$ include temperature dependent fluid properties and cooling through flow rate, Q. Since cooling through flow rate is determined by the charge and back pressures imposed upon the converter, it is not explicitly included in the variable list. The temperature dependent properties of density, ρ, viscosity, μ, specific heat, C_p, and thermal conductivity, k, were all taken at the input temperature of the cooling flow supplied to the torque converter. Equation (1) gives a functional list of the primary

and secondary variables that determine $T_{s,i}$ in an automotive torque converter:

$$T_{s,i} = f(D, L_t, K, TR, n_{sb}, t_{max}, l_c, p_{ave}, \Delta p, \rho, \mu, C_p, k). \quad (1)$$

The dimensionless form of (1) was resolved into dimensionless stator torque as a function of five dimensionless design parameters and two dimensionless operating point parameters using the repeating variables of D, ρ, p_{ave}, and C_p:

$$\frac{T_{s,i}}{D^3 p_{ave}} = f\left(\frac{L_t}{D}, U, TR, n_{sb}, \frac{t_{max}}{l_c}, \frac{\Delta p}{p_{ave}}, Pr\right). \quad (2)$$

The dimensionless design parameters include torus aspect ratio, L_t/D, unit input speed (see Part I), U, stall torque ratio, TR, number of stator blades, n_{sb}, and stator blade thickness ratio, t_{max}/l_c. The dimensionless operating point parameters are dimensionless operating pressure, $\Delta p/p_{ave}$, and the Prandtl number, Pr. These seven dimensionless parameters were used as dimensionless regressors to fit empirical model(s) to dimensionless stator torque.

Not all of the dimensionless design parameters of (2) are necessary when considering a particular population of torque converters. Those dimensionless design parameters that remain constant are removed from (2) before fitting a model to the data. This was the case in Part I, where the dimensions of both torque converters were exactly scaled by the ratio of their diameters. This resulted in U and TR being constant for each diameter along with the design parameters of n_{sb}, and t_{max}/l_c. These dimensionless regressors were subsequently removed from the functional list of (2) before proceeding to fit a model to the data.

2.3. Response surface methodology

Response surface methodology (RSM) and a stepwise regression procedure were used to model the relationship of dimensionless stator torque with the dimensionless design and operating point parameters of (2). The general form of the second-order response surface (RS) assumed for this investigation is given by (3), which includes linear, quadratic, and two-factor interactions:

$$\hat{y} = b_0 + \sum_{i=1}^{k} b_i x_i + \sum_{i=1}^{k} b_{ii} x_i^2 + \sum_{i=1}^{k-1} \sum_{j=i+1}^{k} b_{ij} x_i x_j + \varepsilon. \quad (3)$$

The response, $\hat{y}$, is dimensionless stator torque at cavitation and the linear, quadratic, and two-factor interactions, x_i, x_i^2, and $x_i x_j$, respectively, are the dimensionless regressors of (2). The estimated regression coefficients, b_0, b_i, b_{ii}, and b_{ij} were determined using least squares method. The term, ε, is the residual or error of the model, the difference between the experimentally measured and predicted value of dimensionless stator torque.

A stepwise regression technique was utilized to produce a RS model with the minimum number of dimensionless regressors that are statistically significant with 95% confidence. Equation (4) was the initial form of the RS model

assumed, from which dimensionless regressors are sequentially added based upon meeting the statistical criterion of a 95% joint Bonferroni confidence interval and t-test; see [10]:

$$\hat{y} = b_0 + \varepsilon. \quad (4)$$

During the stepwise regression process, regressors can be added or removed from the model as dictated by the statistical criterion. The overall reduction in error realized by adding any one regressor is dependent upon the regressors already in the model. For a more detailed description of RSM and the stepwise linear regression procedure, the reader is referred to [10, 11].

The accuracy and goodness of fit for any RS model developed were checked by computing the root mean square error (RMSE) and determining the linear association between the dimensionless response and regressors. RMSE is an estimator of a model's standard deviation and for this investigation was computed as a percentage, denoted as %RMSE. Equation (5) defines %RMSE, where y_i is the measured response, n is the number of data points, and p is the number of dimensionless regressors in the model:

$$\%RMSE = \sqrt{\frac{\sum_{i=1}^{n}\left(\left(\left(y_i - \hat{y}_i\right)/y_i\right)*100\right)^2}{n-p}}. \quad (5)$$

A measure of the proportionate amount of variation in the response explained by a particular set of regressors in the model is the adjusted coefficient of multiple determination R_a^2:

$$R_a^2 = 1 - \frac{\sum_{i=1}^{n}\left(y_i - \hat{y}_i\right)^2/n - p}{\sum_{i=1}^{n}\left(y_i - \overline{y}\right)^2/n - 1}. \quad (6)$$

This metric calculates to a value from 0 to 1. Results above 0.85 are generally needed to signify an accurate model of the data set. R_a^2 is typically preferred over R^2, the coefficient of multiple determination, as it is a better evaluator of the number of regressors included in the model. As the number of regressors increases, R^2 will always increase, whereas R_a^2 may increase or decrease depending on whether or not the additional explanatory regressors actually reduce variation in the response. Computationally, the difference between these metrics is that the factors of $n - p$ and $n - 1$ are removed from the numerator and denominator of (6), respectively, to compute R^2.

3. EXPERIMENTAL SETUP AND TEST PROCEDURE

3.1. Dynamometer test cell

The torque converter dynamometer test cell and test procedure used to acquire stator torque cavitation thresholds at stall using nearfield acoustical measurements was described in Part I. A 40 RPM/s stall speed sweep procedure was again utilized to transition all torque converters from a noncavitating to a cavitating condition. Fourteen operating points were applied to each design to characterize their effect on $T_{s,i}$. Table 1 lists the ranges of the three operating points

TABLE 1: Range of stall operating point parameters tested.

Operating point	Low	High
Average pressure	481 kPa	963 kPa
Pressure drop	69 kPa	345 kPa
Input temperature	60°C	80°C

varied in this investigation. The signal processing technique utilized to determine the exact threshold of cavitation was briefly discussed in Part I and further detailed by [8].

3.2. Matrix of experimental torque converters

Four major populations of torque converters were tested with progressively decreasing levels of geometric similitude, as shown in Figure 1 from top to bottom. The first population, referred to as geometric scaling, contains the same torque converters as presented in Part I. The converters maintain exact geometric similitude between diameters. This population served as a baseline comparison for RS models in which geometric similitude was relaxed. The second population, multiple torus geometry, includes three torque converters of similar element design, but varying torus dimensions (D and L_t) to create converters with the same unit input speed, U. The next population consists of multiple pump and stator blade designs, with torus dimensions and turbine design held constant, for 16 total configurations that achieve a range in K-factor performance. The final population includes all converters tested for a total of 51 widely varying designs that encompass a typical design space for powertrain component matching. Within this population, referred to as general torque converter design, geometric similitude was greatly relaxed, allowing the development of a comprehensive RS model capable of predicting $T_{s,i}$. Because of the loosened restrictions on similitude, the resulting model is applicable to general torque converter designs. The details for each population are provided with the discussion of each RS model. The six diameters tested in this investigation will be denoted D_1 through D_6, with D_1 corresponding to the smallest diameter and D_6 to the largest diameter.

4. RESULTS AND DISCUSSION

The RS models developed using the RSM and stepwise regression techniques are presented in the order depicted in Figure 1, from strictest geometric similitude to the most relaxed. The full RS model equations for all of the populations are listed in Table 4, at the end of the paper. It is expected that the RS models presented will be integrated into initial converter design and powertrain component matching to maximize $T_{s,i}$ within a given set of packaging, performance, and stall operating point specifications. Prediction of $T_{s,i}$ during this phase will enable optimization of torus and/or element geometries along with operating pressures and temperature to minimize the effects of cavitation related noise.
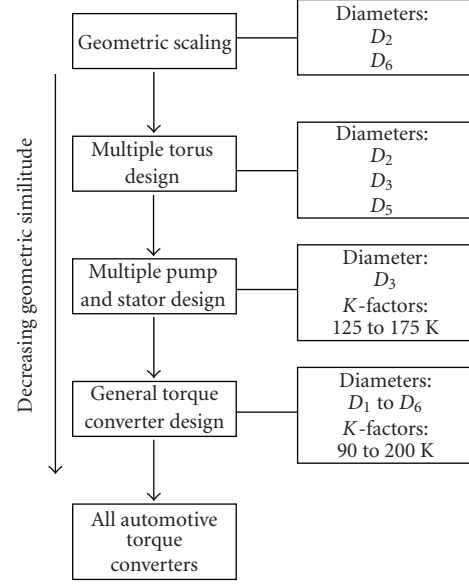

FIGURE 1: Organizational chart for torque converter populations tested; range of converters tested is denoted by diameters and K-factors.
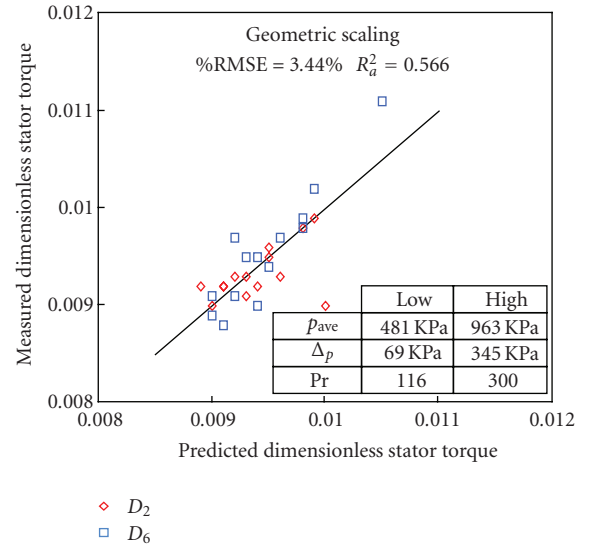

FIGURE 2: Geometric scaling RS model for predicting stator torque at onset of cavitation (28 points).

4.1. Geometric scaling

The cavitation threshold data used to fit the RS model was the same as that used to fit the power product (PP) model of Part I. Equation (7) gives the functional form of the RS model for this population, and the RS model versus test data graph is shown in Figure 2:

$$\frac{T_{s,i}}{D^3 p_{\text{ave}}} = f\left(\frac{\Delta p}{p_{\text{ave}}}, \text{Pr}\right). \tag{7}$$

The model diagnostics (%RMSE and R_a^2) provided in Table 2 show the RS model to have a 23% increase in R_a^2

and a 9% decrease in %RMSE over the corresponding PP model for the same number of dimensionless regressors. Although both models have %RMSE values below 4%, the small R_a^2 values suggest that both models have a low linear association between dimensionless response and regressors. As with the PP model of Part I, a multitude of least squares solutions exists for the geometric scaling data set. Use of dimensionless stator torque results in a nearly constant term for the onset of cavitation over the range of operating points tested. The small variation in dimensionless quantities does not particularly lend itself to empirical modeling, requiring increased variation in dimensionless quantities to adequately define a curve. However, even with relatively low values of R_a^2, the prediction accuracy for scaling stator torque cavitation thresholds for a given torus and set of element designs is high.

4.2. Multiple torus design

For the multiple torus design population, element blade designs were held constant, while the dimensions of the torus were varied for three ratios of L_t/D. Performances for the 3 designs result in equivalent unit input speeds, U. The functional form for this RS model is given by (8) and includes torus aspect ratio and number of stator blades in addition to the terms included in (7):

$$\frac{T_{s,i}}{D^3 p_{\text{ave}}} = f\left(\frac{L_t}{D}, n_{\text{sb}}, \frac{\Delta p}{p_{\text{ave}}}, \text{Pr}\right). \quad (8)$$

The addition of the dimensionless design parameters was required as torus dimensions changed along with some modifications to the stator. The number of stator blades is different between the 3 converters due to differences in axial length, but blade angles are the same. Figure 3 contains the RS model, showing an increase in the range of dimensionless response and regressors compared to the geometric scaling RS model shown in Figure 2. A decrease in model %RMSE from 3.40% to 2.87% and an increase in R_a^2 from 0.566 to 0.925 were realized compared to the geometric scaling model. The multiple torus design RS model includes five regressors, consisting primarily of two factor interactions between dimensionless design and operating point parameters. The utility of this particular model allows prediction of $T_{s,i}$ for a single set of element designs spanning the range of torus dimensions provided in Figure 3.

4.3. Multiple pump and stator design

The dimensionless functional form of the RS model for the population with multiple pump and stator designs is given by

$$\frac{T_{s,i}}{D^3 p_{\text{ave}}} = f\left(U, \text{TR}, n_{\text{sb}}, \frac{t_{\max}}{l_c}, \frac{\Delta p}{p_{\text{ave}}}, \text{Pr}\right). \quad (9)$$

The list of dimensionless regressors includes those that characterize changes to the pump and stator and stall operating point. The converters in this population all have
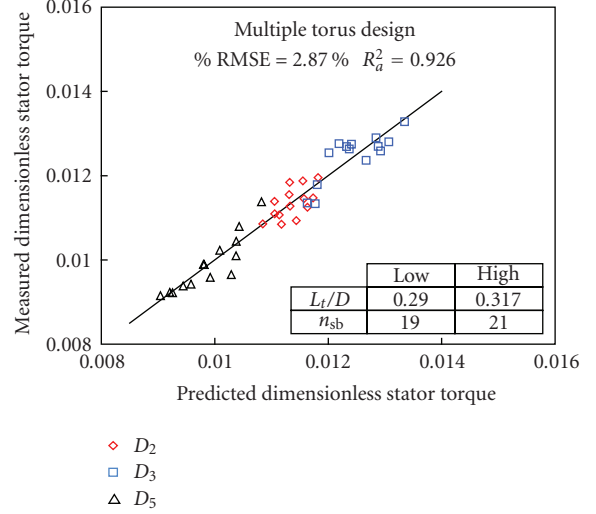

FIGURE 3: Multiple torus design RS model for predicting stator torque at onset of cavitation (42 points).
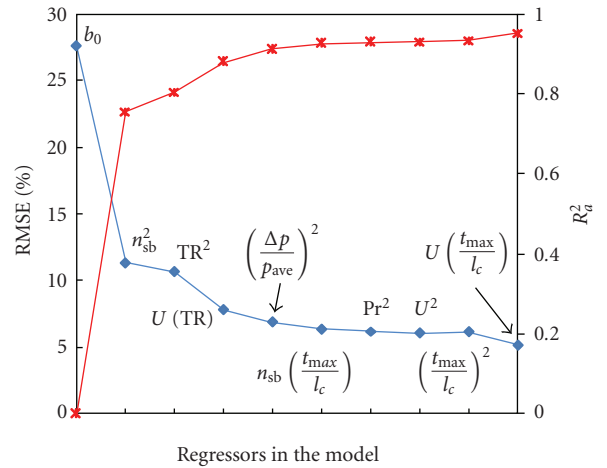

FIGURE 4: Sequential reduction in %RMSE and increase in R_a^2 during stepwise regression procedure for multiple pump and stator design RS model.

TABLE 2: Comparison of geometric scaling models.

Model type	Data points	Regressors	R_a^2	%RMSE
RS	28	2	0.566	3.340
PP	28	2	0.434	3.733

the same torus design, so the L_t/D term included in (8) drops out of (9).

Figure 4 summarizes results from the stepwise regression procedure used to determine statistically significant regressors for the RS model. The figure shows the reduction in model error and an increase in linear association between response and regressors as regressors are added to the model. Only regressors that have a statistically significant effect are retained in the final equation. In this way, the number of
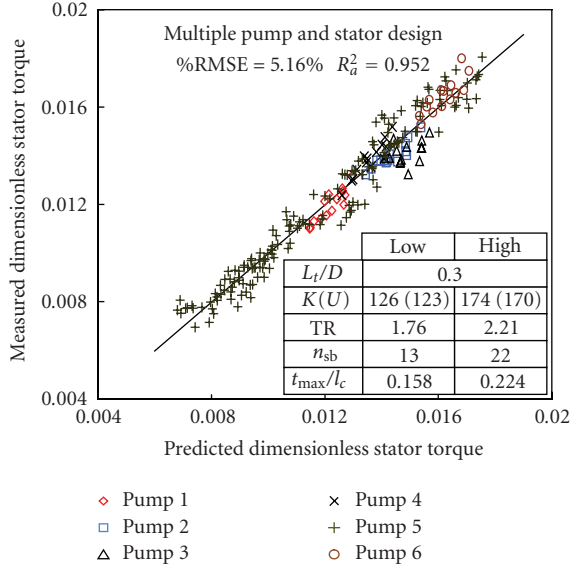
FIGURE 5: RS model for multiple pump and stator design population, data is for 6 pump and 11 stator designs with fixed torus geometry.
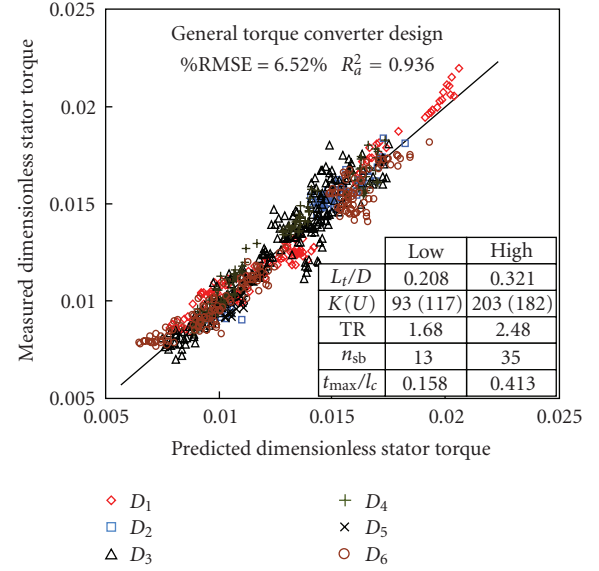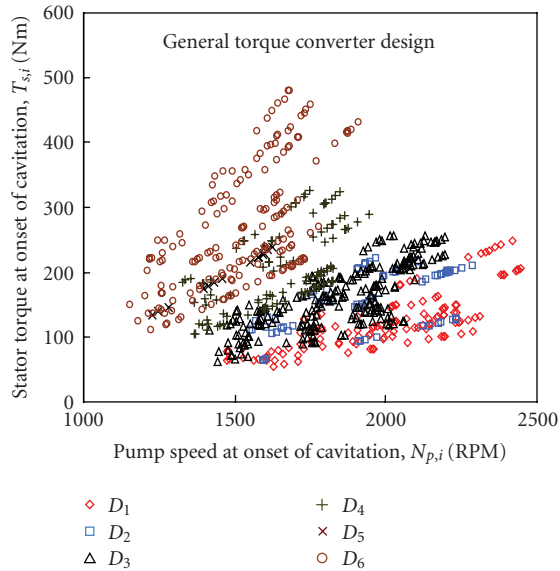

FIGURE 6: Stator torque versus pump speed at onset of cavitation data for 51 widely varying torque converter designs (714 points).

FIGURE 7: RS model for prediction of stator torque at onset of cavitation for general torque converter design.

FIGURE 8: Histogram of residuals for general torque converter design population RS model.

regressors was reduced to 10, from a possible 27, including the constant term, b_0. It can be noted in Figure 4 that the addition of the first three regressors, n_{sb}^2, TR^2, and the interaction $U*TR$ accounts for 88% of the variation in dimensionless stator torque and reduces %RMSE from 27.6% to 7.78%. Building the RS model by sequentially adding dimensionless regressors other than in the order shown in Figure 4 would produce different characteristic values of %RMSE and R_a^2. During the stepwise regression process, models %RMSE and R_a^2 are dependent upon the statistical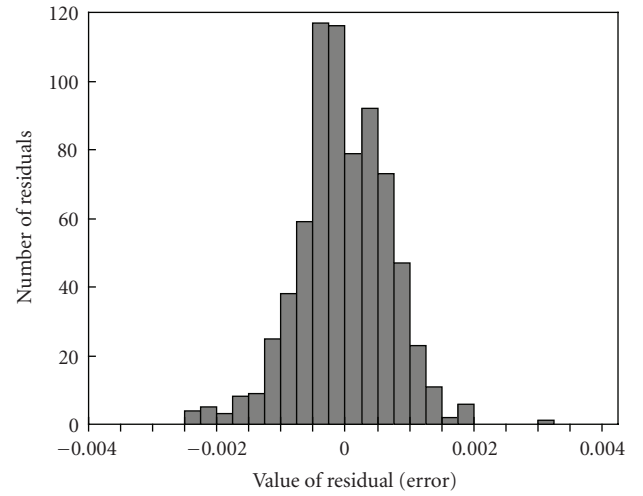 significance of the individual regressor to be added and those regressors already present in the model. For this investigation, regressors were added to the RS model according to their influence on %RMSE and R_a^2. Those regressors, that were deemed statistically significant and generated the highest reduction in %RMSE and increase in R_a^2, were added first. It was found that the regressors based on design parameters produced more statistically significant contributions to reducing model %RSME and increasing R_a^2 than those based on fluid properties, even though cavitation is a fluid dependent phenomenon influenced by pressures and temperatures.

TABLE 3: Comparison of RS model performance by population.

Population	Geometric similitude	Data points	Regressors	R_a^2	%RMSE
Geometric scaling	Exact	28	3	0.566	3.34
Multiple torus design	Elements only	42	6	0.926	2.87
Multiple pump and stator design	Torus only	224	10	0.952	5.16
General torque converter design	None	714	19	0.936	6.52

TABLE 4: Summary of RS models by torque converter population excluding regression coefficients.

Population	Response surface model
Geometric scaling	$\dfrac{T_{s,i}}{D^3 p_{\mathrm{ave}}} = b_0 + b_1\left(\dfrac{\Delta p}{p_{\mathrm{ave}}}\right)^2 + b_2(\mathrm{Pr})^2.$
Multiple torus design	$\dfrac{T_{s,i}}{D^3 p_{\mathrm{ave}}} = b_0 + b_1\left(\dfrac{\Delta p}{p_{\mathrm{ave}}}\right) + b_2\left(\dfrac{L_t}{D}\right)^2 + b_3\left(\dfrac{L_t}{D}\right)\left(\dfrac{\Delta p}{p_{\mathrm{ave}}}\right) + b_4\left(\dfrac{L_t}{D}\right)(\mathrm{Pr}) + b_5(n_{\mathrm{sb}})\left(\dfrac{\Delta p}{p_{\mathrm{ave}}}\right).$
Multiple pump and stator design	$\dfrac{T_{s,i}}{D^3 p_{\mathrm{ave}}} = b_0 + b_1\left(\dfrac{t_{\max}}{l_c}\right) + b_2(U)^2 + b_3(\mathrm{TR})^2 + b_4(n_{\mathrm{sb}})^2 + b_5\left(\dfrac{\Delta p}{p_{\mathrm{ave}}}\right)^2$ $+ b_6(\mathrm{Pr})^2 + b_7(U)(\mathrm{TR}) + b_8(U)\left(\dfrac{t_{\max}}{l_c}\right) + b_9(n_{\mathrm{sb}})\left(\dfrac{t_{\max}}{l_c}\right).$
General torque converter design	$\dfrac{T_{s,i}}{D^3 p_{\mathrm{ave}}} = b_0 + b_1\left(\dfrac{L_t}{D}\right) + b_2(U) + b_3(\mathrm{TR}) + b_4(n_{\mathrm{sb}}) + b_5\left(\dfrac{t_{\max}}{l_c}\right) + b_6\left(\dfrac{L_t}{D}\right)^2 + b_7(n_{\mathrm{sb}})^2 + b_8\left(\dfrac{t_{\max}}{l_c}\right)^2$ $+ b_9\left(\dfrac{\Delta p}{p_{\mathrm{ave}}}\right)^2 + b_{10}(\mathrm{Pr})^2 + b_{11}\left(\dfrac{L_t}{D}\right)(n_{\mathrm{sb}}) + b_{12}\left(\dfrac{L_t}{D}\right)\left(\dfrac{t_{\max}}{l_c}\right) + b_{13}(U)(\mathrm{TR}) + b_{14}(U)(n_{\mathrm{sb}})$ $+ b_{15}(U)\left(\dfrac{t_{\max}}{l_c}\right) + b_{16}(\mathrm{TR})(n_{\mathrm{sb}}) + b_{17}(\mathrm{TR})\left(\dfrac{t_{\max}}{l_c}\right) + b_{18}(n_{\mathrm{sb}})\left(\dfrac{t_{\max}}{l_c}\right).$

The RS model for the multiple pump and stator design population resulting from the stepwise regression is provided in Figure 5. For the 16 different pump and stator combinations included, the RS model has a %RMSE of 5.16% and R_a^2 of 0.952. Compared with the multiple torus geometry RS model, %RMSE increased by 2.29%. This increase is expected as more data points are included, introducing more variation and departing further from geometric similitude. The predicted value of dimensionless stator torque from this RS model can be scaled to other diameters if exact dimensional scaling is observed, and design modifications to pump and stator fall within the scope of the model.

4.4. Generalized torque converter design

A population of converters with variations in both torus and element geometries was utilized to develop a generalized RS model for predicting $T_{s,i}$ at stall. The experimental data, shown in Figure 6 as $T_{s,i}$ versus $N_{p,i}$, pump speed at onset of cavitation, spans a broad range of torques and speeds for the matrix of converters and stall operating points tested.

All of the dimensionless regressors from (2) were used for developing the generalized RS model, as all varied for the matrix of designs tested. The stepwise regression procedure resulted in a RS model with 18 dimensionless regressors and the constant term, b_0. Dimensionless design parameters dominated the reduction in %RMSE and an increase in R_a^2, most notably U, TR, and their interaction. These two regressors along with the constant term reduce %RMSE from 27.76%, for the initial model (4), to 10.36%, and account for 81% of the variation in the dimensionless response. The generalized torque converter RS model for predicting $T_{s,i}$ is shown in Figure 7, differentiated by diameter. The range of design parameters tested are provided, showing the range of torus, stator design specifics, and overall stall performance metrics as determined by element geometries.

The generalized RS model's %RMSE of 6.52% and R_a^2 of 0.936 demonstrates that even with greatly relaxed geometric similitude, an accurate prediction model was developed. Figure 8 is a histogram of the model residuals; the error term defined in (3). It shows that no significant deviations from normalcy and roughly follow that of a normal distribution.

Table 3 compares each RS model developed from a population of torque converters with complete geometric similitude, to populations with diminishing restrictions on geometric similitude. It can be noted that as geometric similitude is relaxed, the number of dimensionless regressors required to realize a highly accurate RS model increases. This is expected as the numerous interactions between design parameters become increasingly important in determining $T_{s,i}$ at stall. The increase in %RMSE occurring sequentially from the geometric scaling to the general torque converter design RS model is not substantial enough to consider RS models lacking geometric similitude to be inaccurate.

Table 4 summarizes the dimensionless regressors that comprise each RS model presented in this paper. In general, the dimensionless regressors found to be most influential in reduction of RS model error reduction are those most closely related to the design and performance characteristics of the turbomachine rather than the dimensionless operating point parameters. Depending on the data set being modeled, the dimensionless design parameter regressors that result in the largest error reduction varied. In the case of the generalized model, the linear terms of unit input speed, U, torque ratio, TR, and their interaction, $U*$TR, were most dominant. Other dimensionless quantities such as torus aspect ratio, number of stator blades, stator blade thickness ratio, and dimensionless operating point serve to explain additional but minor variations in the dimensionless response. The regression coefficients contained in each RS model were determined from proprietary geometries and are withheld from Table 4.

5. CONCLUSIONS

Experimentally obtained values of stator torque at the onset of cavitation for torque converters with varying degrees of geometric similitude were nondimensionalized and used as dimensionless response and regressors for developing response surface (RS) models. A stepwise linear regression procedure reduced the complexity of each RS model by only including statistically significant dimensionless regressors. RS models created from data sets of decreasing geometric similitude showed that R_a^2 values above 0.85 are achieved even with greatly relaxed geometric similitude. The %RMSE values resulting for each RS model of decreasing geometric similitude were not substantial enough to indicate inadequacies in the dimensional analysis or data modeling methodology. A RS model was presented which is capable of predicting $T_{s,i}$ for general automotive torque converter design with a %RMSE of 6.52%. This error is deemed sufficiently low and its scope of prediction large enough to rate the RS model; a valuable tool for optimizing torus and element geometries with respect to the onset of cavitation at stall in three element automotive torque converters.

NOMENCLATURE

C_p: Specific heat (kJ/kg·K)
D: Diameter (m)
K: K-factor (RPM/Nm$^{0.5}$)
L_t: Axial length (m)
$N_{p,i}$: Pump speed at onset of cavitation (RPM)
Pr: Prandtl number
Q: Volumetric flow rate (m^3/s)
R_a^2: Adjusted coefficient of multiple determination
$T_{s,i}$: Stator torque at onset of cavitation (Nm)
TR: Stall torque ratio
U: Unit input speed
%RMSE: Root mean square error (%)
b: Regression coefficients
k: Thermal conductivity (W/m·K)
l_c: Chord length (m)

n_{sb}: Number of stator blades
p_{ave}: Average pressure (Pa)
Δp: Pressure drop (Pa)
t_{max}: Maximum blade thickness (m)
x_i: Dimensionless regressors
$\hat{y}$: Predicted dimensionless response
ε: Residual error
ρ: Density (kg/m^3)
μ: Viscosity (N·s/m^2).
θ_{in}: Input temperature (°C)

REFERENCES

[1] J. I. Madsen, W. Shyy, and R. T. Haftka, "Response surface techniques for diffuser shape optimization," *AIAA Journal*, vol. 38, no. 9, pp. 1512–1518, 2000.

[2] D. Bonaiuti, A. Arnone, M. Ermini, and L. Baldassarre, "Analysis and optimization of transonic centrifugal compressor impellers using the design of experiments technique," *Journal of Turbomachinery*, vol. 128, no. 4, pp. 786–797, 2006.

[3] N. Papila, W. Shyy, L. Griffin, and D. J. Dorney, "Shape optimization of supersonic turbines using global approximation methods," in *Proceedings of the 39th AIAA Aerospace Sciences Meeting and Exhibit*, Reno, Nev, USA, January 2001, paper no. 2001-1065.

[4] N. Papila, W. Shyy, L. Griffin, and D. J. Dorney, "Shape optimization of supersonic turbines using global approximation methods," *Journal of Propulsion and Power*, vol. 18, no. 3, pp. 509–518, 2002.

[5] S. Pierret and R. A. Van den Braembussche, "Turbomachinery blade design using a Navier-Stokes solver and artificial neural network," *Journal of Turbomachinery*, vol. 121, no. 2, pp. 326–332, 1999.

[6] S.-Y. Han, J.-S. Maeng, and D.-H. Yoo, "Shape optimization of cutoff in a multiblade fan/scroll system using response surface methodology," *Numerical Heat Transfer B*, vol. 43, no. 1, pp. 87–98, 2003.

[7] C. J. Fitzgerald, N. R. Weston, Z. R. Putman, and D. N. Mavris, "A conceptual design environment for technology selection and performance optimization for torpedoes," in *Proceedings of the 9th AIAA/ISSMO Symposium on Multidisciplinary Analysis and Optimization*, Atlanta, Ga, USA, September 2002, AIAA 2002-5590.

[8] D. L. Robinette, C. L. Anderson, J. R. Blough, M. A. Johnson, D. G. Maddock, and J. M. Schweitzer, "Characterizing the effect of automotive torque converter design parameters on the onset of cavitation at stall," in *Proceedings of the SAE International Noise and Vibration Conference and Exhibition (SAE '07)*, St. Charles, Ill, USA, May 2007, 2007-01-2231.

[9] G. Venter, R. T. Haftka, and J. H. Starnes, "Construction of response surface approximations for design optimization," *AIAA Journal*, vol. 36, no. 12, pp. 2242–2249, 1998.

[10] M. H. Kutner, C. J. Nachtsheim, and J. Neter, *Applied Linear Regression Models*, McGraw-Hill, New York, NY, USA, 4th edition, 2004.

[11] D. G. Montgomery, *Design and Analysis of Experiments*, John Wiley & Sons, New York, NY, USA, 6th edition, 2005.